Persistent fluctuations of activity in undriven continuum neural field models with power-law connections

C. A. Brackley and M. S. Turner
Department of Physics, University of Warwick, Coventry CV4 7AL, United Kingdom
(Received 20 June 2008; revised manuscript received 30 October 2008; published 22 January 2009)

We study the effect of random inhomogeneous connections on a continuous field description of neural tissue. We focus on a regime in which persistent random fluctuations in activity arise spontaneously in the absence of either time-varying or spatially inhomogeneous input. While present in real tissue and network models of discrete neurons, such behavior has not been reported in continuum models of this type. The activity contains frequencies similar to those seen experimentally. We consider a power-law envelope $r^{-\alpha}$ for the inhomogeneity and present evidence that the statistical coherence (a measure of two-point correlation) rapidly percolates across the system as α is reduced below $\alpha_c \approx 1,2$ in one and two dimensions, respectively.

DOI: 10.1103/PhysRevE.79.011918 PACS number(s): 87.19.ln

INTRODUCTION

Continuum neural field (CNF) models, of the type first proposed by authors such as Wilson and Cowan [1] and Amari [2], have proved to be of enduring interest to theoretical neuroscientists. These models treat neural tissue not as discrete cells, but as a continuous medium, with each point in space characterized by the average membrane potential (or "activity") of cells at that point.

The dynamics of the activity in a general CNF model are governed by the equations

$$\tau_u \frac{\partial u}{\partial t} = -u(\mathbf{x},t) + \int_\Gamma w_{uu}(\mathbf{x},\mathbf{x}') f_u(u(\mathbf{x}',t))d\mathbf{x}' - g \times \int_\Gamma w_{vu}(\mathbf{x},\mathbf{x}') f_v(v(\mathbf{x},t)),$$

$$\tau_v \frac{\partial v}{\partial t} = -v(\mathbf{x},t) + \int_\Gamma w_{uv}(\mathbf{x},\mathbf{x}') f_u(u(\mathbf{x},t)) - g \times \int_\Gamma w_{vv}(\mathbf{x},\mathbf{x}') f_v(v(\mathbf{x},t)), \quad (1)$$

where Γ denotes the extent of the system, and the scalar fields $u(\mathbf{x},t)$ and $v(\mathbf{x},t)$ represent the activity of populations of excitatory and inhibitory neurons, respectively. The "firing rate" functions $f_{u,v}$ describe the conversion between activity and firing rate for each population, and $w_{uu}(\mathbf{x},\mathbf{x}')$, etc. are continuous functions describing the strength of connections between each population from point $\mathbf{x}'$ to point $\mathbf{x}$.

To simplify these equations a number of approximations can be made. Experimentally, it is found that connectivity of inhibitory interneurons is short ranged [3], so we approximate that the inhibitory population only acts locally $w_{vu,uv}(\mathbf{x},\mathbf{x}') \approx \delta(\mathbf{x}-\mathbf{x}')$ and we ignore recurrent inhibition, setting $w_{vv}=0$ [4]. From experiment the firing rate function for a *population* of excitatory cells is known to be of sigmoid form whereas inhibitory cells are found to have an approximately linear response in the phenomenological range of activity [5,6]. We therefore take $f_v(v)=v$ and $f_u(u)=f(u)$, which for analytic tractability we approximate as a step function $f(u)=\Theta(u-\theta)$, where $\Theta(y)=1$ for $y \geqslant 0$, and $\Theta(y)=0$ otherwise. This results in the equations

$$\tau_u \frac{\partial u}{\partial t} + u(\mathbf{x},t) = \int_\Gamma w(\mathbf{x},\mathbf{x}') f(u(\mathbf{x}',t))d\mathbf{x}' - g v(\mathbf{x},t),$$

$$\tau_v \frac{\partial v}{\partial t} + v(\mathbf{x},t) = f(u(\mathbf{x},t)), \quad (2)$$

which we use throughout the rest of this paper, and can be described as a nonlinear negative feedback model [4,7]. The constants g and $\tau_{u,v}$ give the relative strength of the inhibitory population and the response time of the populations, respectively. To reduce the number of free parameters we choose $\tau_u=\tau_v$, this then being the only microscopic relaxation time for the system (this choice does not qualitatively affect our results, and we examine it further in Sec. V and in the supplementary material [8]); the choice $\tau_u=1$ then sets the time units of the system. A recent review of CNF models [7] discusses other variations of this model (for example the "linear feedback" model which we discuss in the Conclusions and in supplementary material [8]), and the solutions they support. These include traveling wave fronts and pulses as well as stationary "bumps" of activity, which have been linked to epileptic seizure [9] and working memory models, respectively. Also, Folias and Bressloff [10] show that, with the addition of external input, stationary activity patterns can go unstable in favor of "breathing" fronts or bumps, and breathers which emit traveling pulses.

A common assumption in previous work on CNF models is that the neural tissue has a connectivity $w(\mathbf{x},\mathbf{x}')$ which is both homogeneous and isotropic in space, using, e.g., highly localized exponential or Gaussian functions of separation $|\mathbf{x}-\mathbf{x}'|$. There is some experimental evidence broadly justifying such choices; for example, Hellwig [11] finds a Gaussian distribution for connections between nearby pyramidal neurons in rat visual cortex. Most studies, however, also show other connections, for example, nonlocal "patchy" connections in visual cortex [12], or heterogeneity in synaptic properties of pyramidal cells in prefrontal cortex [13]. In this paper we address such variation by adding an inhomogeneous component to a Gaussian connection function. Impor-

tantly, such connections would seem to be necessary on general grounds to ensure nontrivial function in neural tissue.

Previous work by Bressloff [14] introduced a particular, periodic inhomogeneity as a short-length-scale modulation of an otherwise homogeneous connection function. Traveling wave front solutions were found to have speed that depended greatly on the length scale of the inhomogeneity. Other work includes [15] where long-range horizontal connections are included in a two-dimensional (2D) model.

In the present work we adopt a more general approach and assume that neural connections are stochastically distributed. The effects of long-range connections are investigated by convoluting a heterogeneous connection function with correlation length λ with a power-law function of separation in both one and two dimensions.

With certain choices of parameters we observe different behavior in a CNF model: spontaneous persistent activity. Broadly speaking, we see distinct regions of the system where activity stays above threshold θ, and regions where it fluctuates about threshold. Fluctuations and persistent activity are phenomena commonly observed in neural systems, e.g., in the various rhythms seen in electroencephalogram (EEG) data. We show here that by inclusion of heterogeneous connections CNF models can exhibit such behavior *without* the need for external input.

I. HETEROGENEOUS CONNECTION FUNCTIONS

We construct our weight function numerically by taking a homogeneous function of separation and adding an inhomogeneous component,

$$w(\mathbf{x},\mathbf{x}') = w_H(|\mathbf{x}-\mathbf{x}'|) + A w_I(|\mathbf{x}-\mathbf{x}'|)[w_1(\mathbf{x}) + w_2(\mathbf{x}')].$$

Here w_H is a simple Gaussian, $w_H(y) = e^{-y^2}/\sqrt{\pi}$, where the integrated weight is normalized to unity, and the unit width sets the length scale of connections in the system. The inhomogeneous envelope is given by

$$w_I(y) = \mathcal{N}\frac{|y|^{-\alpha}}{1+|y|^{-\alpha}}, \tag{3}$$

where α determines the range of the connections, and $\mathcal{N}$ is chosen so that integration of w_I over a system of length L gives unity.

The functions w_1 and w_2 vary randomly in space and are taken to be positive and to have a spatial correlation length λ. We include functions of both $\mathbf{x}$ and $\mathbf{x}'$ in order to remove any bidirectionality; although a connection function that is separable in this manner is a somewhat special case, it nonetheless represents a significant generalization over the more limited connection functions chosen in previous studies (see the Introduction). For simplicity, w_1 and w_2 are chosen to be different realizations of a function with the same statistics, and can loosely be thought to represent additional (to the homogeneous) connections *into* point $\mathbf{x}$ and *out of* point $\mathbf{x}'$. Note that, although the functions are constructed stochastically, they do not vary with time, so the system itself is entirely deterministic; full details of the functions' numerical construction are given in the supplementary information [8].

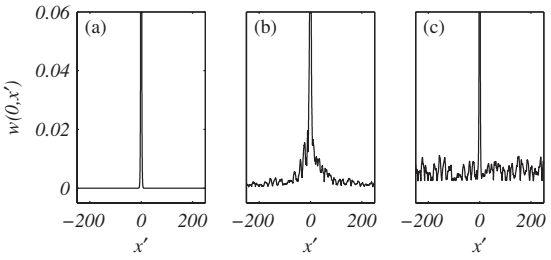

FIG. 1. Typical realizations of the 1D connection function $w(x,x')$ for α=(a) 6, (b) 1, and (c) 0.1. We note that the homogeneous peak of w_H is present in each case. In (c) the long-ranged "tails" of inhomogeneous connection weight have small amplitude due to our normalization; see text.

The inhomogeneity in the connection function is therefore described by the length λ, amplitude A, and exponent α. The regime $\lambda > 1$ corresponds to locally homogeneous connections with inhomogeneous connections more important (less efficiently averaged out) on longer length scales. In the rest of the paper we choose $\lambda=5$ in 1D and $\lambda=3$ in 2D.

Equation (2) is solved by discretizing space and time and using a fourth-order Runge-Kutta routine [16]; the integrals are evaluated using fast Fourier transforms [17] by exploiting the fact that they are of convolution form. In 1D we choose a system size of $L=500$; the 2D simulations are much more computationally expensive, so we choose a smaller square system of side $L=30$. For the rest of this paper for simplicity we fix $\theta=0.1$. Full computational details are given in the supplementary material [8]. Figure 1 shows typical realizations of the connection function for a 1D system with different values of α.

II. SOLUTIONS SUPPORTED BY THE MODEL

Phenomena such as traveling wave fronts occur in homogeneous models due to the fact that the system can be arranged such that there are three uniform steady states $\bar{u}_1 < \bar{u}_2 < \bar{u}_3$, depending on the choice of parameters θ and g. Perturbation about these points shows the lowest ($\bar{u}_1=0$) and the highest ($\bar{u}_3=1-g$) states to be stable. This bistability leads to the existence of traveling front solutions [7]; if a region of the system is in the uppermost steady state, and an adjacent region is in the lowest steady state, then there will be a continuous wave front connecting them. This will travel at a speed determined by θ [18].

Wave front solutions also exist in our model in the large-α (local connection) regime, provided that two steady states exist throughout the system. If stable steady states exist they are given by $\bar{u}(\mathbf{x}) = f(\bar{u})W(\mathbf{x})$, where we define

$$W(\mathbf{x}) = 1 + A\int_\Gamma w_I(\mathbf{x}-\mathbf{x}')[w_1(\mathbf{x}) + w_2(\mathbf{x}')]d\mathbf{x}' - g.$$

If we assume that $W(\mathbf{x}) \geqslant \theta$ for all $\mathbf{x}$, we can still have traveling fronts which connect two steady states (one of which now varies spatially) and propagate at a time-varying speed $c(t)$. If we decrease the value of α below some critical value then, instead of a front propagating at finite speed, u in-

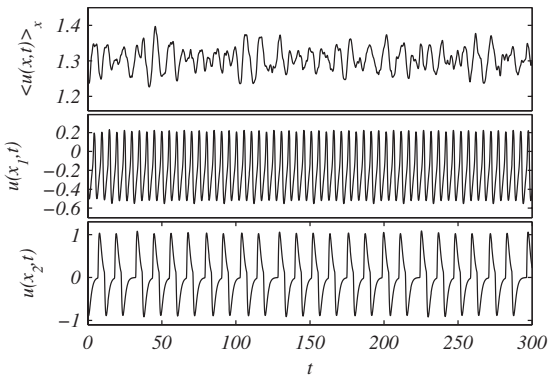

FIG. 2. Activity averaged over all space, $\langle u(x,t)\rangle_x$, and at particular points x_i varying in time. Data here are from a 1D system with $\alpha=6$, $A=1.9$, and $g=2.9$.

creases to its uppermost steady state value at all points in the system.

A different type of behavior is found when $W(\mathbf{x})$ is not greater than θ for all $\mathbf{x}$, i.e., there is only one stable steady state in some regions while there are two in others. In a regime where the inhibition (g) is sufficient to destroy the topmost steady state for some $\mathbf{x}$, we observe persistent fluctuations in $u(x,t)$. The existence of the persistently *fluctuating* state (as opposed to a persistent *stationary* "bump") arises wholly due to the inhomogeneity, and is not possible in the homogeneous model without some sort of external driving.

Figure 2 shows some typical results for $u(x,t)$ in a 1D system with $\alpha=6$ (local connections). Note that if the regions where the topmost steady state exists are not sufficiently spatially extended (i.e., if A is too small or g is too large) then $u\to\bar{u}_1=0$ across the whole system. For consistency we choose g (for given A) such that, in the large-α limit, $W<\theta$ for ~20% of the system (see [8]).

Inspection of the behavior for local connections (large α) shows that there are regions where $u\to 0$ and regions where $u\to W$, with connecting regions where u varies persistently. In regime of long-range connections (small α), we see large regions [where $W(x)>\theta$] in which u fluctuates coherently remaining above θ, with smaller regions where u fluctuates more quickly about θ. Further details and movies of fluctuations in $u(x,t)$ for $\alpha=6$ and $\alpha=0.1$ are available in supplementary material [8].

III. COHERENCE IN FLUCTUATIONS

In order to quantitatively correlate the activity at different points $\mathbf{x}_1$ and $\mathbf{x}_2$ in the system, we use the quantity

$$\gamma^2=\frac{\langle u(\mathbf{x}_1)u(\mathbf{x}_2)\rangle_t^2}{\langle u(\mathbf{x}_1)^2\rangle_t\langle u(\mathbf{x}_2)^2\rangle_t},\tag{4}$$

in which $\langle\cdots\rangle_t$ denotes a time average. Known as the statistical coherence, γ^2 takes the value of 1 if the fluctuations in activity at the two points are identical, and 0 if the fluctuations are independent. If $u(\mathbf{x}_1,t)$ and $u(\mathbf{x}_2,t)$ are both constant in time, one also obtains a large value of γ^2. The variation of this quantity across the system is examined in Figs. 3 (1D) and 4 (2D).

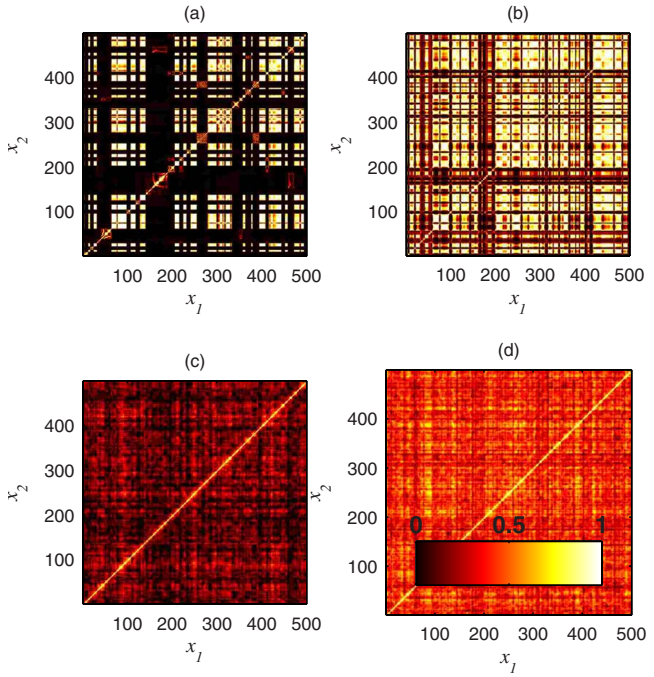

FIG. 3. (Color online) Statistical coherence (4) between points in a 1D system with $A=1.9$ and $g=2.90$. (a) $\alpha=6$ and (b) $\alpha=0.1$ show an average over a single connection function. (c) $\alpha=6$ and (d) $\alpha=0.1$ show averages over ten realizations of the connection function. The color scale for each plot is the same, and is shown bottom right. Note the dramatic percolation of significant statistical coherence away from the diagonal $x_1=x_2$ as α is reduced, increasing the range of the inhomogeneities.

Figure 3(a) shows the coherence between each point in a 1D system with large α. Here the regions with large γ^2 are where $u(x,t)$ is constant in time. Figure 3(c) shows the average of this over ten realizations of the connection function; the regions where u is constant in time are averaged out, and we see that there is little coherence in the fluctuations. Figure 3(b) shows the coherence for small α (long-range connections). Here more of the system exhibits large γ^2, except in

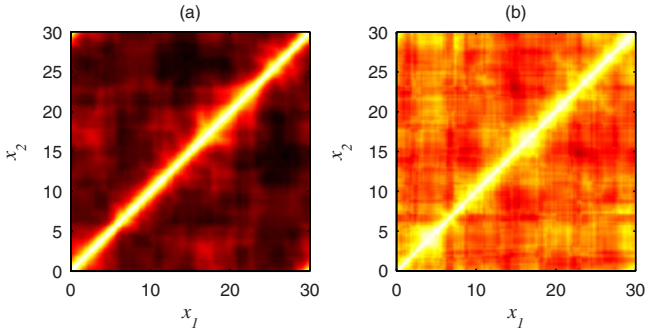

FIG. 4. (Color online) Statistical coherence (4) between points at positions x_1 and x_2 along a random line in a 2D system ($L=30$) with $A=2$ and $g=2.87$, averaged over five realizations of the connections. (a) shows $\alpha=6$ and (b) $\alpha=0.1$. A similar spread in information is observed as α is reduced.

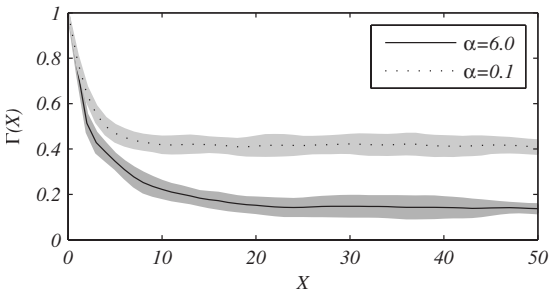

FIG. 5. Average coherence in a 1D system with $A=1.9$ and $g=2.9$ averaged over ten realizations shown as a function of separation for $\alpha=6$ (solid line) and 0.1 (dashed line). One standard deviation variation is shown in the shaded regions. A similar plot for a 2D system is given in the supplementary material [8]. An increase in the range of the correlations as α decreases is clearly visible.

the regions where $u(x,t)$ fluctuates rapidly [where $W(x)<\theta$]. Averaging over ten realizations [Fig. 3(d)] shows much higher coherence than for large α (local connections). Figure 4 shows similar plots for 2D systems; here we randomly choose a line across the system, and look at the coherence between points on that line.

In Fig. 5 we show for the 1D system the average correlation as a function of the distance between two points,

$$\Gamma(X)=\left\langle \frac{\langle u(x,t)u(x-X,t)\rangle_t^2}{\langle u(x,t)^2\rangle_t\langle u(x-X,t)^2\rangle_t}\right\rangle_x \tag{5}$$

where $x=|\mathbf{x}_1|$ and $X=|\mathbf{x}_1-\mathbf{x}_2|$, i.e., we rewrite γ^2 in terms of the spatial separation of points, and average over x. We see that for both large and small α the coherence is large at small separation, and decreases to a plateau as separation increases. At large separations the coherence in approximately four times larger in the long-ranged connection case than in the local connection case.

The difference between the behavior in the long-range and local connection regimes could have large implications for the propagation of information across the system. For long-ranged connections the coherence percolates the system, i.e., we see the entire system behaving coherently.

In Fig. 6 we plot the quantity $\langle[u(\mathbf{x},t)-\langle u(\mathbf{x},t)\rangle_t]^2\rangle_{x,t}$, and we see that this has a large value in the local connection

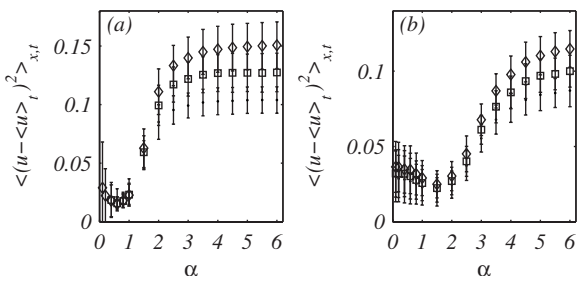

FIG. 6. Quantity $\langle[u(\mathbf{x},t)-\langle u(\mathbf{x},t)\rangle_t]^2\rangle_{x,t}$. Averaged over ten realizations of (a) a 1D system (points, squares, and diamonds show results for $A=1.2$, 1.6, and 1.9, respectively), and (b) a 2D system (points, squares, and diamonds show $A=2$, 2.3, and 2.6, respectively).

regime, and a small value in the long-range regime. We also note that the change is not gradual, but that we can identify a critical value of α. One can see that in the 1D case there is a critical exponent of about $\alpha_c=1$; in the 2D case the change appears more gradual, possibly related to the smaller system size, and occurs between $\alpha=1$ and 3.

IV. ANALYSIS OF THE ROLE OF α

We can better understand the behavior under local connections (large α) by inserting the full connection function into the differential equations (2). If we assume that the function $w_2(\mathbf{x}')$ varies on length scales much longer than the width of the function $w_I(\mathbf{y})$, then we can approximate $w_2(\mathbf{x}')\approx w_2(\mathbf{x})$ and $f(u(\mathbf{x}',t))\approx f(u(\mathbf{x},t))$ in the integrals, giving

$$\frac{\partial u}{\partial t}+u=[1+Aw_1(\mathbf{x})+Aw_2(\mathbf{x})]f(u(\mathbf{x},t))-gv,$$

$$\frac{\partial v}{\partial t}+v=f(u(\mathbf{x},t)). \tag{6}$$

As we have said previously, if $W(\mathbf{x})$ is such that there are some regions where there are two steady states, and somewhere there is only one, then we see persistent fluctuation between the two. The above equations are local in nature, and aside from the case of propagating fronts or pulses, no information is transmitted across the system. The dynamics depend only on the local $W(\mathbf{x})$. Further details of the choice of the other parameters (A, g, etc.) required to give persistent fluctuation are given in the supplementary material [8].

In the opposite regime of long-range connections (small α) we can approximate $w_I(\mathbf{y})$ as a constant ($w_I\sim 1/L$ due to normalization), and the integrals over w_I in Eq. (2) become averages. Thus

$$\frac{\partial u}{\partial t}+u=f(u(\mathbf{x},t))-gv+w_1(\mathbf{x})F_1(t)+F_2(t),$$

$$\frac{\partial v}{\partial t}+v=f(u(\mathbf{x},t)), \tag{7}$$

where $F_1(t)=A\langle f(u)\rangle_x$ and $F_2(t)=A\langle w_2(\mathbf{x})f(u)\rangle_x$.

As described in Sec. II, in this regime there are some regions where u remains above threshold; here $v\to 1$ and $f(u)=1$, so the first two terms on the right-hand side of the equation for u in (7) become constant $1-g$. While $w_1(\mathbf{x})$ varies spatially, F_1 and F_2 show little (or, asymptotically, no) spatial dependence; hence there is large coherence between points in these regions regardless of their separation. In regions where u passes through the threshold θ the first two terms on the right-hand side of the equation for u $[f(u)-gv]$ will also change with time; the fluctuations in these regions is what causes the change in F_1 and F_2, i.e., this drives the fluctuations in the rest of the system.

The difference between the fluctuation in the large- and small-α regimes can be seen in the power spectra of the

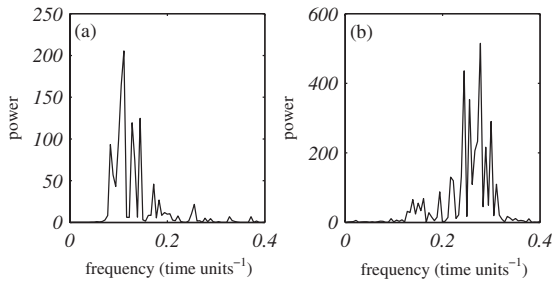

FIG. 7. Power spectra of the mean activity $\langle u(\mathbf{x},t)\rangle_x$ for α=(a) 6 (local connections) and (b) 0.1 (long-range connections). Other parameters are $A=1.9$, $g=2.9$, and $\lambda=5$.

average activity. We define the power as the squared amplitude of each frequency component of the discrete Fourier transform of the time series of $\langle u(\mathbf{x},t)\rangle_x$. Figure 7 shows spectra for $\alpha=0.1$ and 0.6; broadly speaking, fluctuations with frequencies at the *lower* end of this range have the highest amplitudes when the connections are *short* ranged, and vice versa. In both cases we see significant fluctuations at frequencies in the range 0.05–0.3 (time units^{-1}).

V. DISCUSSION

As noted at the start of the paper, our choice $\tau_u=\tau_v$ does not qualitatively affect our results. It does, however, have an influence on the degree to which we see some effects; for example, the difference between the coherence at distant points in the two regimes increases with increasing τ_v. We include a discussion of this with plots similar to Figs. 3 and 5 for different τ_v in the supplementary material.

Another common model is that of linear feedback [19,20], replacing $f(u)\rightarrow u$ in the equation for v in Eq. (2). Rather than an inhibitory population of neurons, the v field in this case could represent spike frequency adaption, synaptic depression, or some other feedback process. We have found that the behavior in the local connection regime is qualitatively the same for both models, but in the long-ranged regime the linear feedback model cannot support persistent fluctuations of this type. We present a plot which shows this in the supplementary material [8].

CONCLUSIONS

We have shown that the introduction of inhomogeneous connections in a continuum neural field model can lead to spontaneous fluctuations, without the need for external input. Such behavior requires a feedback strength g strong enough to destabilize the topmost steady state in some regions of the system. This activity is reminiscent of activity observed in living tissue.

Taking reasonable estimates [5,19] for the length and time parameters (the response time τ_u is of order 10 ms, and the width of w_H is of order 1 mm), we observe significant fluctuations at frequencies in the range 5–30 Hz. This is in the range of frequencies that are observed in real tissue, for example, in theta (4–7 Hz) and alpha (9–11 Hz) rhythms seen in EEG signals [21].

For local connections there is little coherence between the fluctuations in activity at distant points in the system. As we increase the range of the connections, we reach a critical value beyond which the system sharply crosses over to coherent behavior. We identify a critical value of this exponent of $\alpha_c\approx 1$ in the 1D case. In 2D the behavior is qualitatively similar but the critical exponent has a larger value, perhaps $\alpha_c\approx 2$. The sharpness with which information percolates above this threshold may be sensitive to computational limitations on the system size and this makes it more difficult to unambiguously identify the value of α_c in 2D. Coherence in fluctuation in continuum models could be analogous to synchronous firing, which is seen in spiking network models that treat cells individually (for example, [22]).

Finally, we speculate about the significance of the distribution of the most inhomogeneous connections in living tissue. If these are shown to be consistent with power-law connections with exponents *above* α_c then computational activity with a significant spread of mutual information could provide evidence for nonrandomness in these connections.

ACKNOWLEDGMENTS

We gratefully acknowledge stimulating discussions with Magnus Richardson and George Rowlands. We also acknowledge the Centre for Scientific Computing at the University of Warwick for use of desktop and HPC systems.

[1] H. R. Wilson and J. D. Cowan, Kybernetik **13**, 55 (1973).
[2] S. Amari, Biol. Cybern. **27**, 77 (1977).
[3] C. D. Gilbert and T. N. Wiesel, J. Neurosci. **9**, 2432 (1989).
[4] D. J. Pinto and G. B. Ermentrout, SIAM J. Appl. Math. **62**, 226 (2001).
[5] D. A. McCormick, B. W. Connors, J. W. Lighthall, and D. A. Prince, J. Neurophysiol. **54**, 782 (1985).
[6] G. La Camera, A. Rauch, D. Thurbon, H.-R. Lüscher, W. Senn, and S. Fusi, J. Neurophysiol. **96**, 3448 (2006).
[7] S. Coombes, Biol. Cybern. **93**, 91 (2005).
[8] See EPAPS Document No.E-PLEEE8-79-067901 for further details. For more information on EPAPS, see http://www.aip.org/pubservs/epaps.html.
[9] R. D. Chervin, P. A. Pierce, and B. W. Connors, J. Neurophysiol. **60**, 1695 (1988).
[10] S. E. Folias and P. C. Bressloff, SIAM J. Appl. Dyn. Syst. **3**, 378 (2004).
[11] B. Hellwig, Biol. Cybern. **82**, 111 (2000).
[12] P. Buzás, U. T. Eysel, P. Adorján, and Z. F. Kisvárday, J. Comp. Neurol. **437**, 259 (2001).
[13] Y. Wang, H. Markram, P. H. Goodman, T. K. Berger, J. Ma, and P. S. Goldman-Rakic, Nat. Neurosci. **9**, 534 (2006).
[14] P. C. Bressloff, Physica D **155**, 83 (2001).

[15] P. C. Bressloff, Physica D **185**, 131 (2003).
[16] H. Press, S. A. Teukolsky, W. T. Vetterling, and B. P. Flannery, *Numerical Recipes in Fortran*, 2nd ed. (Cambridge University Press, Cambridge, UK, 1992).
[17] M. Frigo and S. G. Johnson, Proc. IEEE **93**, 216 (2005).
[18] C. A. Brackley and M. S. Turner, Phys. Rev. E **75**, 041913 (2007).
[19] P. C. Bressloff, S. E. Folias, A. Prat, and Y. X. Li, Phys. Rev. Lett. **91**, 178101 (2003).
[20] D. J. Pinto and G. B. Ermentrout, SIAM J. Appl. Math. **62**, 206 (2001).
[21] P. L. Nunez and R. Srinivason, *Electric Fields of the Brain—The Neurophysics of EEG*, 2nd ed. (Oxford University Press, Oxford, 2006).
[22] D. Golomb and D. Hansel, Neural Comput. **12**, 1095 (2000).